Quantum Electronics **51** (4) 283–286 (2021)

LASERS

https://doi.org/10.1070/QEL17540

Comparison of AlGaInAs/InP semiconductor lasers (λ = 1450–1500 nm) with ultra-narrow and strongly asymmetric waveguides

N.A. Volkov, V.N. Svetogorov, Yu.L. Ryaboshtan, A.Yu. Andreev, I.V. Yarotskaya, M.A. Ladugin, A.A. Padalitsa, A.A. Marmalyuk, S.O. Slipchenko, A.V. Lyutetskii, D.A. Veselov, N.A. Pikhtin

Abstract. **Semiconductor lasers based on AlGaInAs/InP heterostructures with ultra-narrow and asymmetric waveguides are comparatively studied. It is shown that the use of these waveguides with a simultaneous increase in the quantum well depth makes it possible to increase output powers. Such lasers based on both strongly asymmetric and ultra-narrow waveguides with a stripe contact width of 100 μm demonstrate an output power of 5 W (at pump currents of 11.5 and 14 A, respectively) in a continuous-wave regime at room temperature and a wavelength of 1450–1500 nm.**

Keywords: *semiconductor laser, heterostructure, AlGaInAs/InP, ultra-narrow waveguide, asymmetric waveguide.*

1. Introduction

High-power semiconductor lasers have found wide application in many fields of science and engineering. Among recent works devoted to high-power lasers emitting in the spectral range 1400–1600 nm, we should mention studies on lasers with ultra-narrow [1, 2] and strongly asymmetric [3–6] waveguides. The main specific feature of these designs is a decreased p-waveguide thickness, which reduces optical losses caused by carrier leakage into the waveguide with increasing pump current and improves heat removal from the active region in the case of mounting the crystal with the p-side down [7, 8]. In addition, the output characteristics of lasers of this spectral range can be improved by using strained quantum wells (QWs) to decrease the probability of nonradiative Auger-recombination processes [9–11], as well as by using deeper strain-compensated QWs [12–14] and/or wide-bandgap barriers near the active region [15–18] to decrease the carrier leakage from the active region to the waveguide.

In [2], we compared 1550-nm AlGaInAs/InP lasers with ultra-narrow and broadened waveguides. It was shown that an ultra-narrow waveguide in conjunction with profiled doping, owing to reduced series and thermal resistances and lower optical losses, makes it possible to delay the saturation of the light–current characteristic (LCC) and thus increase the output power by 25%–30%. The study of AlGaInAs/InP lasers with asymmetric and broadened waveguides [19] showed that the use of an asymmetric waveguide allows one to restrict the growth of internal optical losses with increasing pump current and to increase the output power by 1.5 times with respect to the power of lasers with a broadened waveguide. Nevertheless, comparative analysis of two similar approaches based on the use of asymmetric and ultra-narrow waveguides remains topical. These approaches are united by the common idea of decreasing the p-waveguide width, but considerably differ in the n-waveguide parameters and, therefore, in the character of the fundamental optical mode distribution. An additional difference between the considered heterostructures is a larger distance from the active region to the p^+ contacts in lasers with an ultra-narrow waveguide. Due to a weak waveguide, a considerable part of radiation in this structure propagates in the InP emitter layers, which makes it necessary to increase their width. However, despite a higher thermal conductivity of InP in comparison with other compounds of the AlGaInAs/InP material system, an increase in the thickness of InP layers reduces heat removal from the QW, which can affect the laser operation in limiting regimes. At the same time, the asymmetric design makes it possible to redistribute the electromagnetic wave to the side of the n-emitter and shift the QW closer to the heat sink. Unfortunately, the broadened n-waveguide in these lasers is formed using AlGaInAs solid solutions characterized by the worst thermal and transport properties, which may limit the output optical power.

In the present work, we compare the two mentioned approaches (with the use of ultra-narrow and strongly asymmetric waveguides) in order to determine the most efficient way to create high-power semiconductor lasers emitting in the spectral range 1450–1500 nm.

2. Experiment

The AlGaInAs/InP laser heterostructures were grown by MOCVD. We studied two types of heterostructures based on the common idea of narrowing the p-waveguide. The first heterostructure with an ultra-narrow waveguide, which was described in [1, 2], contained the active region consisting of two strain-compensated InGaAs QWs located in the centre of an ultra-narrow AlGaInAs waveguide 0.1 μm thick. The QW parameters were chosen to achieve lasing in the spectral range 1450–1500 nm. The waveguide was sandwiched between InP emitter layers. To decrease leakages, AlInAs barrier layers

N.A. Volkov, V.N. Svetogorov, Yu.L. Ryaboshtan, A.Yu. Andreev, I.V. Yarotskaya, M.A. Ladugin, A.A. Padalitsa Sigm Plus Ltd, ul. Vvedenskogo 3, korp. 1, 117342 Moscow, Russia; e-mail: volkov_n_a@mail.ru;
A.A. Marmalyuk Sigm Plus Ltd, ul. Vvedenskogo 3, korp. 1, 117342 Moscow, Russia; National Research Nuclear University MEPhI, Kashiskoe sh. 31, 115409 Moscow, Russia;
S.O. Slipchenko, A.V. Lyutetskii, D.A. Veselov, N.A. Pikhtin Ioffe Institute, ul. Politekhnicheskaya 26, 194021 St. Petersburg, Russia

Received 16 February 2021
Kvantovaya Elektronika **51** (4) 283–286 (2021)
Translated by M.N. Basieva

isoperiodic with the InP substrate were formed on the waveguide–emitter interface. In the second heterostructure, the p-side of the initially broadened waveguide was decreased so that the QW turned out to be in the immediate vicinity of the p-emitter (similar to the structure described in [3, 4]). The energy band diagrams of the studied heterostructures are presented in Fig. 1. The obtained heterostructures were used to fabricate semiconductor lasers with a stripe contact width of 100 μm and a cavity length of 2000–3000 μm. The cavity faces were coated with antireflection and reflection layers with $R_1 \sim 00.5$ and $R_2 \sim 0.95$. The crystals were mounted onto a copper heat sink, and the output characteristics of the lasers were studied in the cw operation regime at a heat sink temperature of 25 °C.

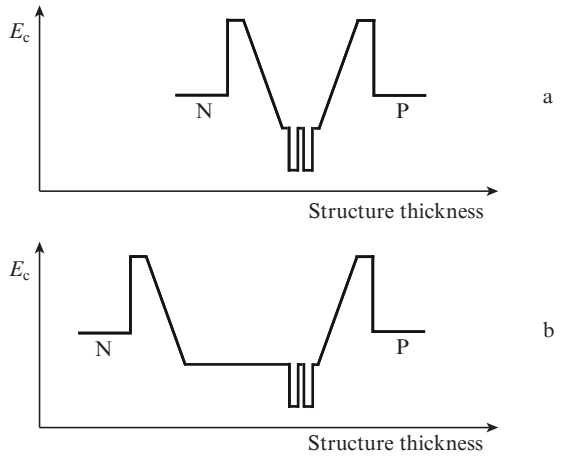

Figure 1. Schematic energy band diagram of the active region of AlGaInAs/InP semiconductor lasers with (a) ultra-narrow and (b) asymmetric waveguides.

3. Results and discussion

The fortunate combination of optical, electrophysical, and thermal parameters allowed one to use AlGaInAs/InP heterostructures with an ultra-narrow waveguide to develop highly efficient semiconductor lasers emitting in the spectral range 1400–1600 nm. A decrease in the thickness of AlGaInAs waveguide layers, which have high series and thermal resistances, positively affects the thermal load on the active region at high pump currents and can diminish accumulation of charge carriers in the p-waveguide, which restricts the growth of internal optical losses, delays the LCC saturation, and makes it possible to achieve a higher output power. At the same time, the approach with use of an ultra-narrow waveguide in the InGaAs/GaAs/AlGaAs and AlGaAs/GaAs heterostructures turned out to be not so successful because these lasers did not demonstrate any increase in the output powers in comparison with the lasers based on the same heterostructures with a conventional broadened waveguide [20–22]. This indicates a restricted applicability of this approach due to the parameters of the used materials.

On the other hand, the variant with the use of an asymmetric waveguide attracts attention due to the possibility of positioning the active region closer to the heat sink and thus retaining the advantages of a narrow p-waveguide. In the InGaAs/GaAs/AlGaAs material system, lasers of this design demonstrated higher output characteristics than the lasers with emitters based a broadened waveguide [23–25].

For more complete comparison of these approaches to the development of lasers emitting in the spectral range 1400–1500 nm, the parameters of heterostructures were chosen so that the optical confinement factors of the active region were similar. The compositions of waveguide layers, the geometries, and the energy depth of QWs were identical. Since the p-waveguide thicknesses in the studied structures coincided, we hoped to observe similar characters of carrier leakage and accumulation in both waveguides. It was expected that the studied lasers will have different levels of internal optical losses and different characters of LCC saturation with increasing pump current.

The LCCs and the dependence of their slopes on the pump current for the studied lasers are given in Figs 2 and 3. One can see that, while the threshold currents of both laser types are almost the same, the LCC slopes (slope efficiencies) of these lasers in the initial range are different and remain unchanged to a current of 3 A for the asymmetric-waveguide laser and to 4.3 A for the laser with an ultra-narrow waveguide. The LCC slope for the laser with an ultra-narrow waveguide is smaller, which is related to higher internal optical losses due to penetration of part of the electromagnetic wave into the emitter region. The latter effect can be partially compensated by profiled doping of the structure. Nevertheless, due to a better heat removal from the active region, lasers with an ultra-narrow waveguide can operate at higher pump currents and are characterised by a slower decrease in the LCC slope (Fig. 3). The maximum optical power for the samples with asymmetric and ultra-narrow waveguides was 5 W, but this value was achieved at different working currents. In particular, the laser with an asymmetric waveguide demonstrated this power at a current of 11.5 A, and the laser with an ultra-narrow waveguide reached this power at 14 A. The stripe contact width of both lasers was 100 μm, and the cavity length was 2000 μm. The dependences of the LCC slopes on the pump current intersected at a current of about 10 A (Fig. 3). Although the lasers with an asymmetric waveguide have a larger slope efficiency in the initial LCC region than the lasers with an ultra-narrow waveguide, the output power of the former more rapidly saturates with increasing pump current.

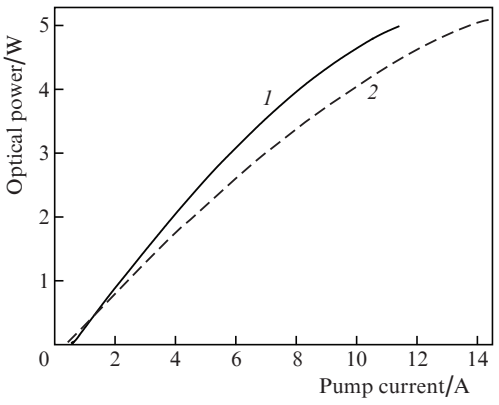

Figure 2. Light–current characteristics of semiconductor lasers based on AlGaInAs/InP heterostructures with (*1*) asymmetric and (*2*) ultra-narrow waveguides in the cw operation regime.

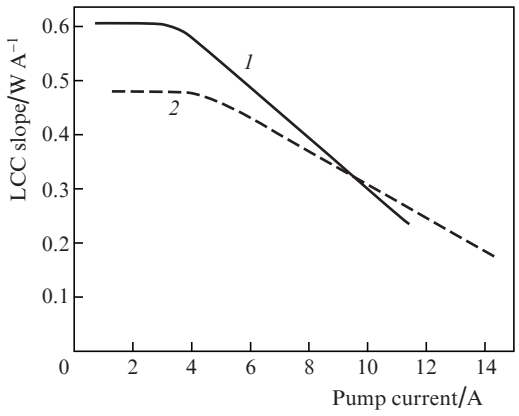

Figure 3. LCC slope vs. the pump current for lasers based on AlGaInAs/InP heterostructures with (*1*) asymmetric and (*2*) ultra-narrow waveguides in the cw operation regime.

The transparency current density (J_0 = 120–150 A cm^{-2}) and the internal quantum efficiency (η_i = 0.93–0.96) of the studied lasers were close, while the level of internal optical losses in the laser with an asymmetric waveguide was predictably lower (α_i = 1.0–1.5 cm^{-1}) than that of the sample with an ultra-narrow waveguide (α_i = 2.0–2.5 cm^{-1}). Figure 4 presents the experimental dependences of the inverse slope efficiency on the cavity length of the studied samples, which allowed us to determine the internal quantum yield and internal optical losses.

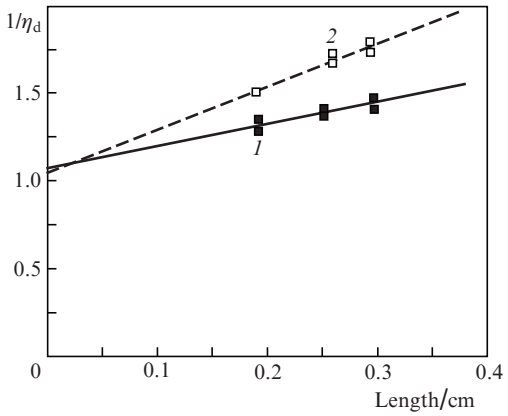

Figure 4. Dependences of inverse slope efficiency η_d on the cavity length of lasers based on AlGaInAs/InP heterostructures with (*1*) asymmetric and (*2*) ultra-narrow waveguides.

The wavelength of the studied lasers was in the range 1450–1500 nm depending on the pump level (Fig. 5). The difference in the slopes of the curves indicates a higher thermal load on the active region of the laser with an asymmetric waveguide compared to the laser with an ultra-narrow waveguide. This result well agrees with the dependences of the LCC slope on the pump current for the studied lasers.

The far-field FWHM divergence in the plane perpendicular to the p–n junction was 40–43° for the lasers with an asymmetric waveguide and 30–32° for the lasers with an ultra-narrow waveguide; the divergence in the plane parallel to the p–n junction was 7–9° and 10–12°, respectively.

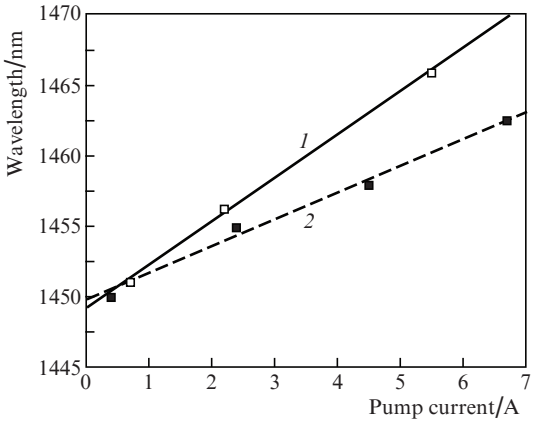

Figure 5. Dependences of the wavelength of semiconductor lasers based on AlGaInAs/InP heterostructures with (*1*) asymmetric and (*2*) ultra-narrow waveguides on the pump current in the cw operation regime.

In this work, we showed that a decrease in the waveguide thickness form one side (shift of the active region to the p-emitter) and two sides (ultra-narrow waveguide) makes it possible to increase the laser power in comparison with the power of conventional structures with a broad waveguide. The creation of conditions for decreasing carrier accumulation in the p-waveguide and improving heat removal from the active region allowed us to increase the maximum achievable laser power to 5 W in the cw regime at a wavelength of 1450–1500 nm for both laser types. Lasers with an asymmetric waveguide demonstrate a higher slope efficiency, which, however, faster decreases with increasing pump current. From this point of view, lasers with an ultra-narrow waveguide, whose output characteristics can be improved by decreasing internal optical losses, seem more advantageous.

4. Conclusions

In this work, we presented the results of comparative experimental study of semiconductor lasers based on AlGaInAs/InP heterostructures with waveguides of different designs. The shift of the QW to the p-emitter in a strongly asymmetric waveguide reduces accumulation of carriers in the p-waveguide and improves heat removal, whilea simultaneous increase in the QW depth improves electron localisation in the active region and increases the differential quantum efficiency. The structure with an ultra-narrow waveguide mainly retains the mentioned advantages of the structure with an asymmetric waveguide but is characterised by higher internal losses due to significant penetration of the electromagnetic wave into the emitter layers (the latter effect was partially compensated by profiled doping). All this allowed us to increase the output power of the studied lasers with both waveguide types to 5 W in the cw regime.

Acknowledgements. This work was partially supported by the National Research Nuclear University MEPhI (Moscow Engineering Physics Institute) Academic Excellence Project (Agreement No. 02.a03.21.0005).

References

1. Marmalyuk A.A., Ryaboshtan Yu.L., Gorlachuk P.V., Ladugin M.A., Padalitsa A.A., Slipchenko S.O., Lyutetskii A.V., Veselov D.A., Pikhtin N.A. *Quantum Electron*., **47**, 272 (2017) [*Kvantovaya Elektron*., **47**, 272 (2017)].
2. Marmalyuk A.A., Ryaboshtan Yu.L., Gorlachuk P.V., Ladugin M.A., Padalitsa A.A., Slipchenko S.O., Lyutetskii A.V., Veselov D.A., Pikhtin N.A. *Quantum Electron*., **48**, 197 (2018) [*Kvantovaya Elektron*., **48**, 197 (2018)].
3. Gorlachuk P.V., Ivanov A.V., Kurnosov V.D., Kurnosov K.V., Marmalyuk A.A., Romantsevich V.I., Simakov V.A., Chernov R.V. *Quantum Electron*., **48**, 495 (2018) [*Kvantovaya Elektron*., **48**, 495 (2018)].
4. Bagaeva O.O., Danilov A.I., Ivanov A.V., Kurnosov V.D., Kurnosov K.V., Kurnyavko Yu.V., Marmalyuk A.A., Romantsevich V.I., Simakov V.A., Chernov R.V. *Quantum Electron*., **49**, 649 (2019) [*Kvantovaya Elektron*., **49**, 649 (2019)].
5. Hallman L.W., Ryvkin B.S., Avrutin E.A., Aho A.T., Viheriala J., Guina M., Kostamovaara J.T. *IEEE Photonics Technol. Lett*., **31**, 1635 (2019).
6. Ryvkin B.S., Avrutin E.A., Kostamovaara J.T. *Semicond. Sci. Technol*., **35**, 085008 (2020).
7. Ryvkin B.S., Avrutin E.A. *J. Appl. Phys*., **100**, 023104 (2006).
8. Veselov D.A., Shashkin I.S., Bakhvalov K.V., Lyutetskii A.V., Pikhtin N.A., Rastegaeva M.G., Slipchenko S.O., Bechvai E.A., Strelets V.A., Shamakhov V.V., Tarasov I.S. *Semiconductors*, **50**, 1225 (2016) [*Fiz. Tekh. Poluprovodn*., **50**, 1247 (2016)].
9. Lui W.W., Yamanaka T., Yoshikuni Y., Seki S., Yokoyama K. *Appl. Phys. Lett*., **64**, 1475 (1994).
10. Wang J., von Allmen P., Leburton J-P., Linden K.J. *IEEE J. Quantum Electron*., **31**, 864 (1995).
11. Andreev A.D., Zegrya G.G. *Semiconductors*, **31**, 297 (1997) [*Fiz. Tekh. Poluprovodn*., **31**, 358 (1997)].
12. Lin C-C., Liu K-S., Wu M-C., Shiao H-P. *Jpn. J. Appl. Phys*., **37**, 3309 (1998).
13. Pan J-W., Chen M-H., Chyi J-I. *J. Cryst. Growth*., **201/202**, 923 (1999).
14. Wu M-Y., Yang C-D., Lei P-H., Wu M-C., Ho W-J. *Jpn. J. Appl. Phys*., **42**, L643 (2003).
15. Kazarinov R.F., Belenky G.L. *IEEE J. Quantum Electron*., **31**, 423 (1995).
16. Takemasa K., Munakata T., Kobayashi M., Wada H., Kamijoh T. *IEEE Photonics Technol. Lett*., **10**, 495 (1998).
17. Abraham P., Piprek J., DenBaars S.P., Bowers J.E. *Jpn. J. Appl. Phys*., **38**, 1239 (1999).
18. Garrod T., Olson D., Klaus M., Zenner C., Galstad C., Mawst L., Botez D. *Appl. Phys. Lett*., **105**, 071101 (2014).
19. Volkov N.A., Andreev A.Yu., Yarotskaya I.V., Ryaboshtan Yu.L., Svetogorov V.N., Ladugin M.A., Padalitsa A.A., Marmalyuk A.A., Slipchenko S.O., Lyutetskii A.V., Veselov D.A., Pikhtin N.A. *Quantum Electron*., **51**, 133 (2021) [*Kvantovaya Elektron*., **51**, 133 (2021)].
20. Malag A., Jasik A., Teodorczyk M., Jagoda A., Kozłowska A. *IEEE Photonics Technol. Lett*., **18**, 1582 (2006).
21. Hung C.-T., Lu T.-C. *IEEE J. Quantum Electron*., **49**, 127 (2013).
22. Bobretsova Yu.K., Veselov D.A., Klimov A.A., Vavilova L.S., Shamakhov V.V., Slipchenko S.O., Pikhtin N.A. *Quantum Electron*., **49**, 661 (2019) [*Kvantovaya Elektron*., **49**, 661 (2019)].
23. Bogatov A.P., Gushchik T.I., Drakin A.E., Nekrasov A.P., Popovichev V.V. *Quantum Electron*., **38**, 935 (2008) [*Kvantovaya Elektron*., **38**, 935 (2008)].
24. Hasler K.H., Wenzel H., Crump P., Knigge S., Maasdorf A., Platz R., Staske R., Erbert G. *Semicond. Sci. Technol*., **29**, 045010 (2014).
25. Kaul T., Erbert G., Klehr A., Maaßdorf A., Martin D., Crump P. *IEEE J. Sel. Top. Quantum Electron*., **25**, 1501910 (2019).